Field emission from carbon nanotube arrays fabricated by pyrolysis of iron phthalocyanine

2004 J. Phys. D: Appl. Phys. 37 5

(http://iopscience.iop.org/0022-3727/37/1/002)

INSTITUTE OF PHYSICS PUBLISHING JOURNAL OF PHYSICS D: APPLIED PHYSICS
J. Phys. D: Appl. Phys. **37** (2004) 5–9 PII: S0022-3727(04)65735-4

Field emission from carbon nanotube arrays fabricated by pyrolysis of iron phthalocyanine

Jiaohua Song, Mingyan Sun, Qing Chen, Jingyun Wang, Gengmin Zhang[1] and Zengquan Xue

Department of Electronics, School of Electronics Engineering and Computer Science, Peking University, Beijing 100871, People's Republic of China

Received 8 July 2003
Published 10 December 2003
Online at stacks.iop.org/JPhysD/37/5 (DOI: 10.1088/0022-3727/37/1/002)

Abstract
Arrays of multi-walled carbon nanotubes (MWCNTs) were fabricated by pyrolysis of iron phthalocyanine (FePc). A silicon wafer and a stainless steel plate were used as the substrates. MWCNTs grown on the silicon wafer were packed closely to each other and were thus well aligned, while those grown on the stainless steel plate had a low density and were oriented randomly. Field emission was achieved from the MWCNT arrays on both substrates. The turn-on electric fields of the silicon-based and stainless steel-based arrays were measured to be 1.9 V μm^{-1} and 3.4 V μm^{-1}, respectively. The emission site distribution was also studied using a transparent anode. The field emission from the MWCNTs on the silicon substrate occurred mainly at the edge regions, while that from the MWCNTs on the stainless steel substrate exhibited a much better uniformity. We attribute this disparity in the emission site distribution to the screening effect of the electric field.

1. Introduction

Carbon nanotubes (CNTs) are considered to have great potential for application in future flat panel displays (FPDs) due to their promising field emission performance (De Heer *et al* 1995, Bonard *et al* 1998a, Kim *et al* 2000). However, many difficulties still remain to be overcome before this object can be eventually achieved. One of them is to work out a method of fabricating large-area CNT arrays conveniently at a relatively low cost. A chemical vapour deposition (CVD) method was developed by utilizing nickel phthalocyanine (NiPc) as the vapour source (Yudasaka *et al* 1997). More recently, synthesis of pillar-shaped structures and patterns of three-dimensional CNT arrays were achieved by pyrolysis of iron phthalocyanine (FePc) (Wang *et al* 2001a, 2002). The simplicity of this method lies in the fact that the metal phthalocyanines used in the synthesis simultaneously provide both the carbon source and the metallic catalysts that are needed in the formation of CNTs. Although quartz is considered very suitable for CNT growth (Yudasaka *et al* 1997, Wang *et al* 2001b), it is an insulator and hence inappropriate for field emission studies. Fortunately, CNTs have also been grown on different conducting substrates using this approach (Araki *et al* 1999). However, within our knowledge, it is still unclear whether multi-walled carbon nanotube (MWCNT) arrays fabricated by pyrolysis of metal phthalocyanines are indeed suitable for field emission applications.

In this context, we have fabricated CNT arrays by pyrolysis of FePc on silicon wafers and stainless steel plates and studied their field emission properties.

2. Sample fabrication

The CNT arrays were fabricated in a quartz tube that was of 1.3 m length, 27 mm inner diameter and 3 mm thickness. The quartz tube was inserted into two furnaces that are in series. A mixed gas of argon and hydrogen with a 1 : 1 volume ratio and a 60–70 cm^3 min^{-1} flow rate was introduced into the tube from one end, and it flowed out from another. A 0.15 g of the FePc source material was placed in the furnace upstream of the flowing gas. The substrate, either a p-type silicon wafer or a stainless steel plate, was placed in the furnace downstream. The upstream furnace was kept

[1] Author to whom any correspondence should be addressed.

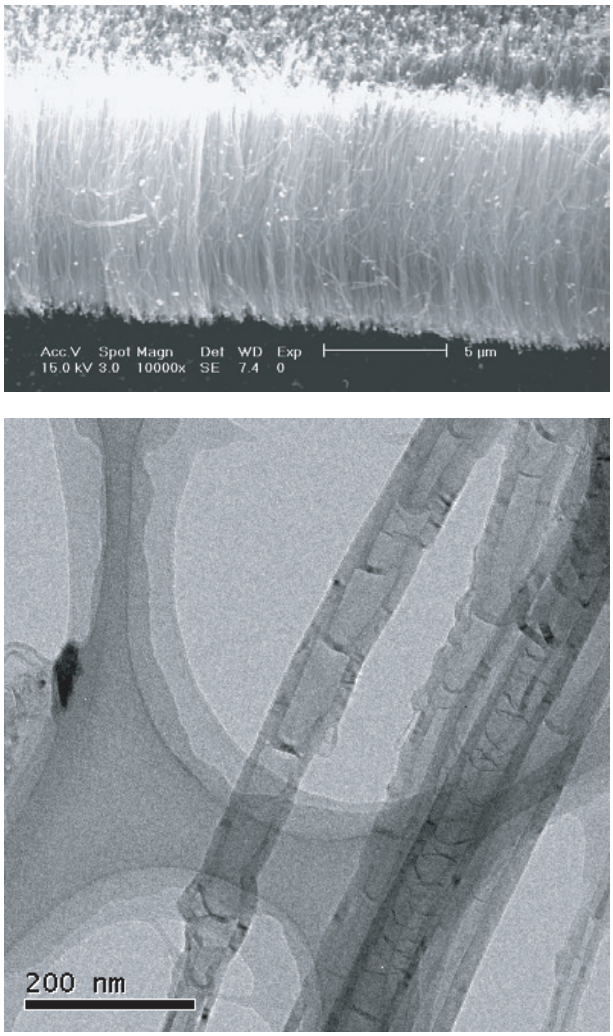

Figure 1. The CNTs grown on the Si substrate: (*a*) an SEM image; (*b*) a TEM image.

at 650–750˚C, the sublimation temperature of FePc, and simultaneously the downstream furnace was kept at 850˚C, the pyrolysis temperature of FePc. This first stage was allowed to last 10 min. Then the temperature of the upstream furnace was also raised to 850˚C, so that the whole furnace was kept at the temperature for the pyrolysis of FePc. This second stage also lasted 10 min. Then the heater was switched off and the sample was allowed to cool down to room temperature in the furnace with the gas still flowing through the tube. The samples obtained were examined using an FEI XL F30 scanning electron microscope (SEM) and an FEI Tecnai 20 transmission electron microscope (TEM).

An array of vertically aligned CNTs was grown on the silicon substrate, as shown in figure 1(*a*). The CNTs are all packed close to each other, with the distance between two neighbouring CNTs being less than 100 nm. This high density is believed to be responsible for the good alignment. Nevertheless, as will be shown below, such a high density might constitute a hindrance to obtaining satisfactory field emission uniformity (Nilsson *et al* 2000). The CNTs were all uniformly about 8 μm in length.

As shown in figure 1(*b*), the CNTs were all MWCNTs, and their diameters ranged from 10 to 50 nm. The CNTs

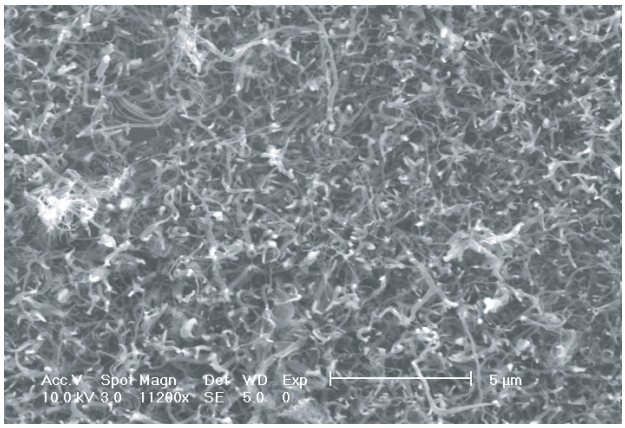

Figure 2. An SEM image of the MWCNTs grown on the stainless steel substrate.

in the figure have a bamboo-shaped structure, which is in agreement with the previous works in which metallic catalysts were used (Li *et al* 1999, Zhang *et al* 2001). Generally, a nanometre-scale metallic particle has a much lower melting point than does its bulk state (Baffat 1976). According to the model put forward by Zhang *et al* (2001), the emergence of a bamboo-shaped structure results from the collective interaction between the surface diffusion of carbon, the convection inside the liquid iron particles and the capillary sucking of the liquid iron particles into the CNTs. Therefore, the bamboo-shaped structure shown in figure 1(*b*) confirms that metallic iron particles were generated in the pyrolysis of FePc and played a key role in the CNT formation. It is consequently safe to argue that in our experiment the pyrolysed FePc indeed provided both the carbon atoms and the catalysts that are necessary for the CNT growth.

As shown in figure 2, we also managed to grow MWCNTs on the stainless steel plate, and a different configuration was attained. Compared with the MWCNTs grown on the silicon wafer, those grown on the stainless steel plate were distributed rather sparsely and had a random orientation. Their average diameter was around 40 nm.

Regarding the mechanism of CNT growth by FePc pyrolysis, we tentatively use the interpretation offered by Araki *et al* (1999). The surfaces of metals such as iron, nickel and stainless steel are unfavourable for the formation of nanometre-scale catalyst particles, which are believed to be indispensable for the commencement of CNT growth. Consequently, there exist far more growth sites on the silicon wafer than on the stainless steel plate and thus the disparity in the CNT density resulted.

3. Field emission from the MWCNT arrays

The field emission measurement was carried out in a home-made metallic ultrahigh vacuum system, whose base pressure was maintained at 10^{-7} Pa by a sputter-ion pump. The sample grown on the silicon substrate, 32 mm^2 in area, was adhered to a molybdenum plate and used as the cathode. A glass screen covered by a tin oxide film, onto which a layer of fluorescent powder had been deposited beforehand, served as the anode. This ‘transparent anode technique’ allowed us to observe

the spatial distribution of the emission sites on the cathode (Xu *et al* 1993). The field emission surface was separated from the anode by 0.5 mm using a spacer. An external steady-voltage source was used to apply a voltage of up to several thousand volts between the anode and the cathode. Field emission currents below 5 μA were measured with a small-current amplifier and those above 5 μA were acquired with micro ammeters of different ranges. When necessary, surface cleaning was performed using a tungsten filament behind the cathode through thermal radiation.

3.1. Field emission from the MWCNT array grown on the silicon substrate

Field emission was achieved from the MWCNT array grown on the silicon substrate, and the current versus voltage curves (I–V curves) are shown in figure 3.

First, before the sample received any heat treatment, an I–V curve was acquired. The turn-on field under which a 10 μA cm^{-2} current density is extracted (Bonard *et al* 1998b) was determined to be 1.4 V μm^{-1}. Limited by the output power of our voltage source, the generally defined threshold current density, 10 mA cm^{-2} (Bonard *et al* 1998b), was not achieved in our measurement. Since some researchers have argued that a current density of 1 mA cm^{-2} could also meet the requirement of some actual applications (Lee *et al* 2002), we use this value as the definition of the threshold current density here. It can be seen from curve 1 that the current density reached this threshold at the 2.6 V μm^{-1} electric field. Despite the low turn-on and threshold fields, the field emission was rather unstable. On average a 15% fluctuation was observed in the measurements. It is generally believed that at this moment the field emission is still dominated by the adsorbates on the CNTs.

Then the sample was heated to 400°C for about 40 min, and curve 2 was acquired after the heating. This time the field emission became much more stable. The fluctuation was below 5%. Simultaneously, however, the turn-on and threshold fields rose to 1.9 V μm^{-1} and 3 V μm^{-1}, respectively. The components of the released gases during the heat treatment were monitored using a quadrupole mass spectrometer. The principal desorbed gas component was water vapour, which is generally believed to result in a large but unstable field emission from CNTs (Zhang *et al* 2002).

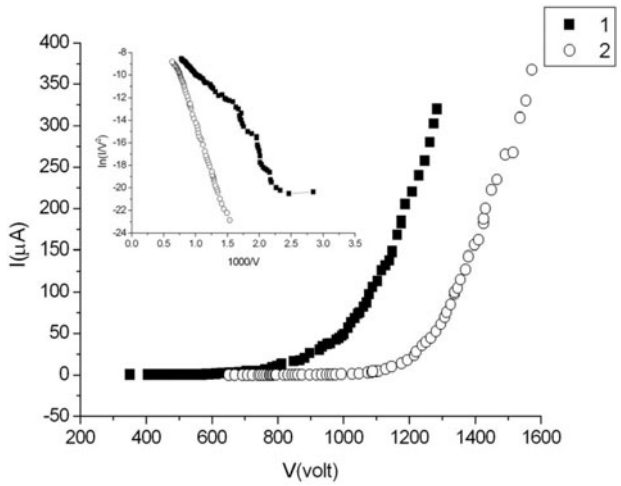

Figure 3. The field emission from the MWCNT array grown on the silicon substrate. Curve 1: before any heat treatment. Curve 2: after heating at 400°C.

Although it is a very crude approximation, the Fowler–Nordheim (FN) formula (Fowler and Nordheim 1928) is still frequently used as a mathematic interpretation of field emission from different nanowires:

$$J = \frac{1.56 \times 10^{-6} E^2}{\phi} \exp\left(-\frac{6.83 \times 10^7 \phi^{3/2}}{E}\right),$$

where J is the field emission current density in A cm^{-2}, ϕ the work function in eV and E the local electric field at the emission sites in V cm^{-1}. The actual value of E could not be measured directly, and it is related to the applied voltage, V, by setting $E = \beta V/d$, where d is the anode–cathode separation and β is the so-called enhancement factor of the field. β depends on the emitter geometry and, for tip-like structures, can be determined by the aspect ratio of the emitter (Filip *et al* 2001). In the following part of this paper, the electric field directly calculated by V/d is termed the 'apparent electric field', so that it can be distinguished from the actual local field, $E = \beta V/d$, at the emission sites. Although the field emission from CNTs probably has a more profound mechanism than that the FN theory is based on, the I–V behaviour of the MWCNTs under our investigation seemed to follow the FN formula well, as suggested by the inset of figure 3. According to the FN theory, β can be computed from the slope of an FN curve if the work function of the tip is known. The lack of an energy analyser made a direct determination of the work function impossible in our experiment. Tentatively, we have to use the value of bulk graphite, 5 eV (Chen *et al* 1998). We would like to point out that by doing so we probably have overestimated the work function of the MWCNTs; thus the calculated β could be higher than the actual one. Under this assumption, β is calculated to be 2×10^3. We think a field enhancement of the order of 10^2 should be more reasonable.

If the cathode had been submitted to heat treatment at higher temperatures, a further change in field emission properties might have been observed. Nonetheless, for fear that the strong thermal radiation from the heated cathode might evaporate the fluorescent powder on the transparent anode, we did not raise the heating temperature to higher values.

Besides low turn-on and threshold voltages, uniformly distributed emission sites with a high density are also a necessity of an ideal field emitter to be used in FPDs (Kuo *et al* 2002). Therefore, we observed the two-dimensional spatial distribution of the emission sites on the cathode using a transparent anode. The result is shown in figure 4.

It can be found that most of the emission sites were located at the periphery of the sample, which is not so conducive for practical use. When nanowires are too close to each other, a screening effect weakens the field enhancement at the tips of individual nanowires. It has been reported that the screening effect cannot be neglected as long as the inter-nanowire distance is smaller than twice the nanowire length (Nilsson *et al* 2000). As shown in figure 1, the MWCNTs grown on the silicon substrate are all packed close to each other. Hence, the local field at the tips of the individual MWCNTs must have been seriously reduced. At the edge regions, however, the screening came from one side only and

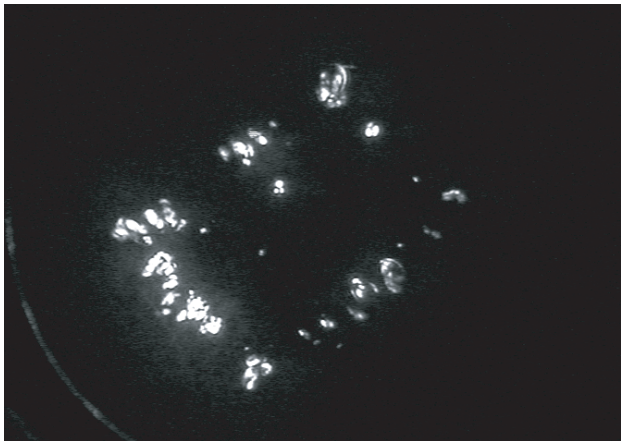

Figure 4. Emission site distribution of the MWCNT array grown on the silicon substrate.

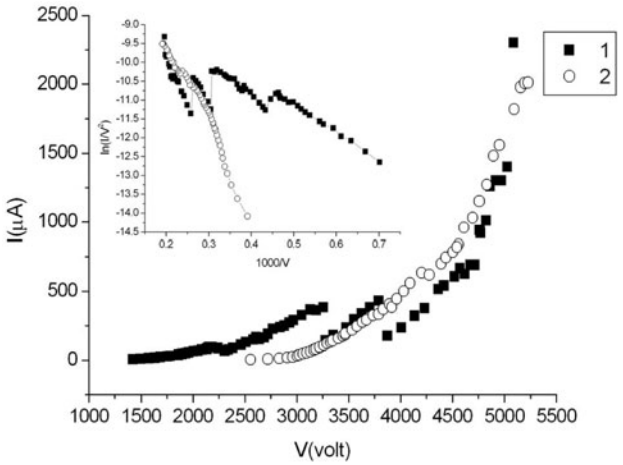

Figure 5. The field emission from the MWCNT array grown on the stainless steel substrate. Curve 1: before any heat treatment. Curve 2: after heat treatment.

is thus expected to become weaker. As a result, these edge regions made the major contribution to the field emission.

The emission site density (ESD) of the cathode plane under a 2 V μm^{-1} apparent electric field is estimated to be 4×10^2 cm^{-2}. The accuracy of this result is limited by the resolution of the CCD camera and the overlapping of the spots on the fluorescent screen. What is more, the significance of this result is qualified by the fact that it is an area-dependent average density over the whole cathode plane. The local ESD of the periphery is calculated to be over 1×10^3 cm^{-2}.

3.2. Field emission from the MWCNT array grown on the stainless steel substrate

The field emission properties of the MWCNT array grown on the stainless steel plate were studied in the same way. This time the array was 1 cm^2 in area and the anode–cathode separation was 0.8 mm.

I–V curves, as shown in figure 5, were acquired before and after heat treatment. Curve 1 features two abrupt tumbles in the current, which were accompanied by a simultaneous deterioration of the degree of vacuum. As pointed out above, at this moment adsorbates were still playing the key role, and hence desorption at a relatively high field and large current resulted in the sudden drop in field emission current. As expected, a heat treatment around 400°C, during which water vapour was the main component of the released gases, stabilized the field emission and a smooth *I–V* curve resulted. The turn-on and threshold fields were determined to be 3.4 V μm^{-1} and 5.9 V μm^{-1}, respectively.

The field enhancement factor, β, is calculated to be 3×10^3 if the work function is supposed to be 5 eV again.

Many researchers have reported good field emission properties from nonaligned CNTs (Collins and Zettl 1997, Chen *et al* 1998, Küttel *et al* 1998, Bonard *et al* 1998a). Though no definite consensus has been reached on the emission mechanism, the imperfections on the flank walls of the CNTs are usually considered responsible for the field emission (Chen *et al* 2000). We speculate that these imperfections are prone to the generation of local states and field enhancement. The former could provide electron reservoirs and the latter could lead to a high field; consequently, strong field emission occurs

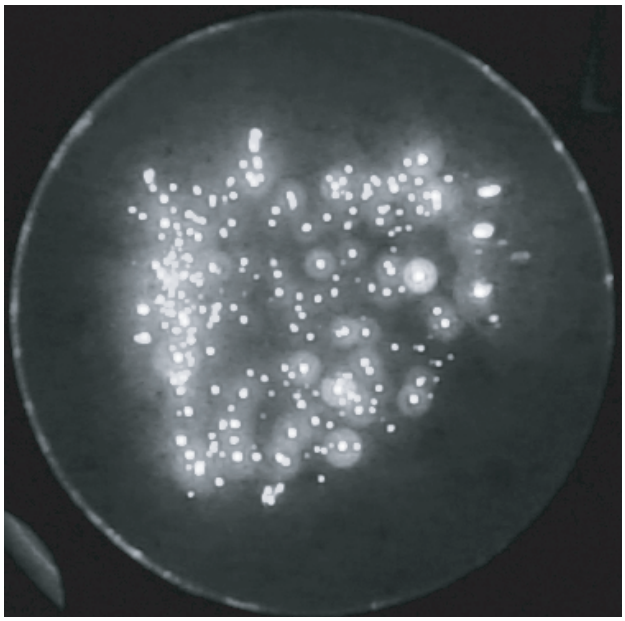

Figure 6. Emission site distribution of the MWCNT array grown on the stainless steel substrate.

easily. Figure 2 shows that the CNTs deposited on the stainless steel plate are all more or less bent, suggesting the existence of such imperfections as pentagons, heptagons and 'bamboo nodes' on the flank walls. Furthermore, we believe that the CNT ends also contributed to the field emission.

A pattern of the emission site distribution in the stainless steel-based MWCNT array was imaged on the transparent anode, as shown in figure 6. The distribution was much more uniform than that of the silicon-based MWCNT array. A straightforward explanation is that the screening effect became much less considerable in the low-density MWCNT array, and thus the MWCNTs in the entire cathode surface, instead of the periphery only, could participate in the field emission.

The ESD was estimated to be 3×10^2 cm^{-2} at a 2 V μm^{-1} apparent electric field. It increased with the applied anode–cathode voltage until the apparent field became fairly high. As

the apparent field was raised to about $3\,\mathrm{V}\,\mu\mathrm{m}^{-1}$, the whole screen emanated light, and the emission sites were hardly distinguishable from each other. The ESD at this moment was estimated to have reached $\sim 10^3$.

An ESD of the order of 10^3 has been reported from both CNT field emitters (Küttel *et al* 1998) and other carbonaceous materials (Pan *et al* 1997, Hart *et al* 1999). Generally, in the latter case, the apparent field required is much higher. In this sense, the CNT emitters have an edge over the emitters based on other carbonaceous materials.

4. Conclusion

MWCNT arrays were grown on both a silicon wafer and a stainless steel plate by pyrolysis of FePc. The MWCNTs grown on the silicon substrate had a high density and good alignment. In contrast, those grown on the stainless steel substrate exhibited a much lower density. In our experiment, although the silicon substrate was obviously more favourable for MWCNT growth, it was the stainless steel substrate that yielded a better performance in field emission. We attribute this disparity to the strong screening effect in the silicon-based sample. Our results suggest that a large-area array of vertically aligned CNTs with a high density is not appropriate for FPD applications because of the screening effect. Moreover, for practical applications, the fabrication temperature of the CNT arrays has to be lowered to below 500–600°C (Talin *et al* 2001). Therefore, our next step is to search for a fabrication process that may be performed at a relatively low temperature and produces CNT arrays with an optimal density.

Acknowledgments

Mr Guili Xiao set up the system for the field emission measurement. Mr Xingyu Zhao took the pictures of the emission sites imaged on the transparent anode. Professor Zhaoxiang Zhang, Dr Renchao Che and Mr Liang Chen offered valuable advice and help in our work. The work was supported by the National Natural Science Foundation of China (Nos 60271004, 60171025 and 60128101).

References

Araki H, Kajii H and Yoshino K 1999 *Japan. J. Appl. Phys.* **38** L1351
Baffat P A 1976 *Thin Solid Films* **32** 283
Bonard J M, Salvetat J P, Stöckli T, de Heer W A, Forró L and Châtelain A 1998a *Appl. Phys. Lett.* **73** 918
Bonard J M, Maier F, Stöckli T, Châtelain A, de Heer W A, Salvetat J P and Forró L 1998b *Ultramicroscopy* **73** 7
Chen Y, Patel S, Ye Y, Shaw D T and Guo L P 1998 *Appl. Phys. Lett.* **73** 2119
Chen Y, Shaw D T and Guo L P 2000 *Appl. Phys. Lett.* **76** 2469
Collins P G and Zettl A 1997 *Phys. Rev.* B **55** 9391
De Heer W A, Châtelain A and Ugarte D 1995 *Science* **270** 1179
Filip V, Nicolaescu D, Tanemura D and Okuyama F 2001 *Ultramicroscopy* **89** 39
Fowler R H and Nordheim L W 1928 *Proc. R. Soc. Lond. Ser.* A **119** 173
Hart A, Satyanarayana B S, Milne W I and Robertson J 1999 *Appl. Phys. Lett.* **74** 1594
Kim J M, Choi W B, Lee N S and Jung E J 2000 *Diamond Relat. Mater.* **9** 1184
Kuo M T, May P W and Ashfold M N R 2002 *Diamond Relat. Mater.* **11** 1422
Küttel O M, Groening O, Emmenegger C and Schlapbach L 1998 *Appl. Phys. Lett.* **73** 2113
Lee C J, Lee T J, Lyu S C, Zhang Y, Ruh H and Lee H J 2002 *Appl. Phys. Lett.* **81** 3648
Li Y D, Chen J L, Ma Y M, Zhao J B, Qin Y N and Chang L 1999 *Chem. Commun.* **12** 1141
Nilsson L, Groening O, Emmenegger C, Kuettel O, Schaller E, Schlapbach L, Kind H, Bonard J M and Kern K 2000 *Appl. Phys. Lett.* **76** 2071
Pan L S, Felter T E, Ohlberg D A A, Hsu W L, Fox C A, Cao R and Vergara G 1997 *J. Appl. Phys.* **82** 2624
Talin A A, Dean K A and Jaskie J E 2001 *Solid-State Electron.* **45** 963
Wang X B, Liu Y Q and Zhu D B 2001a *Chem. Commun.* **8** 751
Wang X B, Liu Y Q and Zhu D B 2001b *Chem. Phys. Lett.* **340** 419
Wang X B, Liu Y Q and Zhu D B 2002 *Adv. Mater.* **14** 165
Xu N S, Tzeng Y and Latham R V 1993 *J. Phys. D: Appl. Phys.* **26** 1776
Yudasaka M, Kikuchi R, Ohki Y and Yoshimura S 1997 *Carbon* **35** 195
Zhang G M, Zhang Z X, Zhang H, Sun J P, Hou S M, Zhao X Y, Liu W M, Xue Z Q, Shi Z J and Gu Z N 2002 *Appl. Surf. Sci.* **195** 20
Zhang X X, Li Z Q, Wen G H, Fung K K, Chen J L and Li Y D 2001 *Chem. Phys. Lett.* **333** 509